Journal of Physics: Condensed Matter

Benchmark of correlation matrix renormalization method in molecule calculations

IOP Publishing Journal Title
Journal XX (XXXX) XXXXXX https://doi.org/XXXX/XXXX

Benchmark of Correlation Matrix Renormalization Method in Molecule Calculations

Han Zhang[1], Wen-Cai Lu[1], Yong-Xin Yao*[, 2], Cai-Zhuang Wang[2] and Kai-Ming Ho[2]

[1] College of Physics and State Key Laboratory of Bio-Fibers and Eco-Textiles, Qingdao University, Shandong 266071, P. R. China
[2] Ames Laboratory-US DOE and Department of Physics and Astronomy, Iowa State University, Ames, Iowa 50011, United States

* Corresponding author E-mail: ykent@iastate.edu

Received xxxxxx
Accepted for publication xxxxxx
Published xxxxxx

Abstract

We report benchmark calculations of the correlation matrix renormalization (CMR) approach for 23 molecules in the well-established G2 molecule set. This subset represents molecules with spin-singlet ground state in a variety of chemical bonding and coordination environments. The QUAsi-atomic Minimal Basis-set Orbitals (QUAMBOs) are used as local orbitals in both CMR and full configuration interaction (FCI) calculations for comparison. The results obtained from the calculations are also compared with available experimental data. It is shown that the CMR method produces binding and dissociation energy curves in good agreement with the QUAMBO-FCI calculations as well as experimental results. The CMR benchmark calculations yield a standard deviation of 0.09 Å for the equilibrium bond length and 0.018 Hartree/atom for the formation energy, with a gain of great computational efficiency which scales like Hartree-Fock method.

Keywords: Electron correlation, First principles, Gutzwiller

1. Introduction

First-principles calculation of strongly-correlated electron materials remains a grand challenge. The strong electron correlation effects drive the systems beyond descriptions of the normal Landau Fermi liquid picture [1, 2], where commonly used density functional theory (DFT) excels. The multi-reference nature of the ground-state many-body wave function in strongly-correlated electron systems also renders the (single-reference) quantum chemistry "gold standard" coupled-cluster method at single and double excitation level broken down [3-5]. Multi-determinant-based quantum chemistry methods, such as multi-reference coupled-cluster [6], multi-configuration self-consistent field, FCI and multi-reference CI [7-9], could be very accurate. However, these methods are limited to samll molecules due to the rapid increase in complexity of the many-body wave function as size of the system increase. Quantum Monte Carlo (QMC) method has achieved impressive progress, especially with the aid of massive parallelization in supercomputers [10-14]. The applications to real correlated materials have been demonstrated [15], but generally it is computationally still very demanding. Meanwhile, hybrid approaches which combines DFT with many-body techniques, such as DFT+onsite Coulomb interaction [16, 17], DFT+dynamical mean-field theory [18-20], and DFT+Gutzwiller method [21-26], have been shown to be very successful in describing real correlated materials. However, the inclusion of adjustable screened Coulomb parameters limits the predictive power of the hybrid methods. Moreover, the question of how to subtract the double-counting term from the DFT-related local onsite correlation contributions remains open and still under active investigations [27-31].

Recently, we have proposed a highly efficient ground state approach for electronic structure and total energy calculations of strongly correlated electron systems without using adjustable Coulomb parameters, namely, the correlation matrix renormalization (CMR) method [32-35]. The CMR method adopts Gutzwiller variational wave function (GWF) to calculate the expectation value of the *ab initio* many-electron Hamiltonian describing the physical system, and follows the idea of commonly used Gutzwiller approximation in the evaluation of both the one-particle density matrix and two-particle correlation matrix [36-39]. The Gutzwiller approximation allows the expectation value of the many-electron Hamiltonian based on GWF in our CMR method to be evaluated with much reduced computational complexity. The computational efforts of the CMR method therefore scale as N^4 or better with respect to the number of basis-set orbitals N, like Hartree-Fock. Moreover, CMR method has no double counting issues in evaluating the total energy. As shown in previous studies and will be shown in the benchmark calculations to be presented in this paper, CMR method can produce fairly accurate binding energy curves of various molecules especially at the bond-breaking and longer inter-atomic distances which are notoriously difficult to deal with due to the strong electron correlation effects.

In our previous work [33], we presented the details of the CMR method for both molecular and periodic systems, including a simplified general form of the orbital renormalization factors and sum-rule corrections as the improvement in formulations. The good accuracy of the CMR method has also been demonstrated in several molecules, one-dimensional linear hydrogen chain and three-dimensional hydrogen atomic crystals, with a comparison to experiments or highly accurate numerical calculations, such as FCI and QMC.

While the details of the CMR theory, formalism, and some of its application have been presented previously, the aim of this work is to make a relatively more comprehensive assessment of the CMR method through benchmark calculations of a subset of molecules with spin-singlet ground state, from the G2 test set. The G2 molecules set was first established by Pople and collaborators and are widely accepted to assess new theoretical methods [40]. The CMR calculations for higher spin-multiplet states are possible and will be presented in a follow-up publication. We will show that the CMR method produces binding and dissociation energy curves in good agreement with FCI calculations as well as experimental results.

The rest of the paper proceeds with a brief review of the CMR method, followed by the benchmark calculation results and discussions of the G2 subset of molecules. Finally, we give a summary and some perspective on the future development of the CMR method.

2. Methods

In the form of second quantization, the full *ab initio* non-relativistic Hamiltonian for an interacting many-electron system can be expressed as

$$H = \sum_{i\Gamma} \mathrm{E}_{i\Gamma} |\Gamma_i\rangle\langle\Gamma_i| + \sum_{i\alpha j\beta,\sigma}' t_{i\alpha j\beta}\, c^{\dagger}_{i\alpha\sigma} c_{j\beta\sigma} + \frac{1}{2} \sum_{\substack{i\alpha j\beta \\ k\gamma l\delta,\sigma\sigma'}}' u\,(i\alpha j\beta; k\gamma l\delta) c^{\dagger}_{i\alpha\sigma} c^{\dagger}_{j\beta\sigma'} c_{l\delta\sigma'} c_{k\gamma\sigma} \qquad (1)$$

where i, j, k, l are the atomic site indices, α, β, γ, δ refer to orbital indices, and σ, σ' indicate the spin indices. Here, t is the one-electron hopping integral expressed as

$$t_{i\alpha j\beta} = \langle \phi_{i\alpha} | \hat{T} + \hat{V}_{ion} | \phi_{j\beta} \rangle \qquad (2)$$

where $\hat{\mathrm{T}}$ and $\hat{\mathrm{V}}_{ion}$ are the operators for kinetic energy and electron-ion interaction, and u is the two-electron Coulomb integral expressed as

$$u(i\alpha j\beta; k\gamma l\delta) = \int dr \int \mathrm{d}r'\, \phi^*_{i\alpha}(\mathrm{r}) \phi^*_{j\beta}(\mathrm{r}') \hat{\mathrm{U}}(|\mathrm{r} - \mathrm{r}'|) \phi_{l\delta}(r') \phi_{k\gamma}(r) \qquad (3)$$

with the Coulomb interaction operator $\hat{\mathrm{U}}$. In eq.(1), the first term is a spectral representation of site-wise local Hamiltonian, in which $\{\Gamma_i\}$ are eigenstates of the local onsite many-body Hamiltonian $\mathrm{H}_{i,\mathrm{loc}}$, which can be written as

$$\mathrm{H}_{i,\mathrm{loc}} = \sum_{\alpha\beta} t_{i\alpha i\beta}\, c^{\dagger}_{i\alpha\sigma} c_{i\beta\sigma} + \frac{1}{2} \sum_{\alpha\beta\gamma\delta,\sigma\sigma'} u(i\alpha i\beta; i\gamma i\delta)\, c^{\dagger}_{i\alpha\sigma} c^{\dagger}_{i\beta\sigma'} c_{i\delta\sigma'} c_{i\gamma\sigma} \qquad (4)$$

$E_{i\Gamma} \equiv \langle \Gamma_i | \mathrm{H}_{i,\mathrm{loc}} | \Gamma_i \rangle$ is the energy of the local configuration $|\Gamma_i\rangle$. The second and third terms in eq. (1) describe the nonlocal one- and two-body contributions, respectively. Σ' means that the pure local on-site terms are excluded from the summation.

The ground state many-body wave function in the CMR approach is approximated by the Gutzwiller variational wave function, which is constructed based on a non-interacting wave function $|\Psi_0\rangle$

$$|\Psi_G\rangle = \prod_i \left(\sum_{\Gamma} \mathrm{g}_{i\Gamma} |\Gamma_i\rangle\langle\Gamma_i| \right) |\Psi_0\rangle, \qquad (5)$$

where $\{\mathrm{g}_{i\Gamma}\}$ are the Gutzwiller variational parameters. Due to strong electron correlations, the local onsite configuration weight can deviate significantly from the mean-field value determined by non-interacting wavefunction Ψ_0. Therefore, the key Gutzwiller parameters $\{g_{i\Gamma}\}$ are introduced to optimize the occupation probability of the local configuration $\{\Gamma_i\}$ in response to electron correlations.

The total energy in CMR thus has the following form

$$E_{\mathrm{CMR}} = E_{\mathrm{loc}} + E_{nl}^{(1)} + E_{nl}^{(2)} + E_{\mathrm{sr}}, \qquad (6)$$

with

$$E_{\mathrm{loc}} = \sum_{i\Gamma} \mathrm{E}_{i\Gamma} p_{i\Gamma}, \qquad (7)$$

$$E_{nl}^{(1)} = \sum_{i\alpha j\beta,\sigma}' t_{i\alpha j\beta} \langle c_{i\alpha\sigma}^{\dagger} c_{j\beta\sigma} \rangle_{\mathrm{G}}, \qquad (8)$$

$$E_{nl}^{(2)} = \frac{1}{2} \sum_{\substack{i\alpha j\beta \\ k\gamma l\delta,\sigma\sigma'}}' u(i\alpha j\beta; k\gamma l\delta) \langle c_{i\alpha\sigma}^{\dagger} c_{j\beta\sigma'}^{\dagger} c_{l\delta\sigma'} c_{k\gamma\sigma} \rangle_{\mathrm{G}}, \qquad (9)$$

$$E_{\mathrm{sr}} = \frac{1}{2} \sum_{i\alpha j\beta,\sigma\sigma'} \lambda_{i\alpha} \left(\langle \hat{n}_{i\alpha\sigma} \hat{n}_{j\beta\sigma'} \rangle_G - N_e \langle \hat{n}_{i\alpha\sigma} \rangle_G \right). \qquad (10)$$

Here N_e is the total number of electrons. The expectation value of a generic operator $\hat{O}$ with respect to the Ψ_{G} is abbreviated as $\langle \hat{O} \rangle_G \equiv \langle \Psi_{\mathrm{G}} | \hat{O} | \Psi_{\mathrm{G}} \rangle$, and similarly for $\langle \hat{O} \rangle_0 \equiv \langle \Psi_0 | \hat{O} | \Psi_0 \rangle$.

Following the kinetic energy renormalization idea of the Gutzwiller approximation (GA) [36, 38-39], the single-electron density matrix is evaluated approximately as

$$\langle c_{i\alpha\sigma}^{\dagger} c_{i\beta\sigma} \rangle_{\mathrm{G}} \approx z_{i\alpha\sigma}^{j\beta} \langle c_{i\alpha\sigma}^{\dagger} c_{i\beta\sigma} \rangle_0, \qquad (11)$$

with $z_{i\alpha\sigma}^{j\beta} = z_{i\alpha\sigma} z_{j\beta\sigma}$ if $(i\alpha) \neq (j\beta)$ and 1 otherwise. Within the CMR approach, the orbital renormalization factor has the form of $z_{i\alpha\sigma} = \sqrt{z_{i\alpha\sigma}^{GA}}$ based on the exact analytical solution of hydrogen dimer. Here $z_{i\alpha\sigma}^{GA}$ is the renormalization factor by the conventional Gutzwiller approximation,

$$z_{i\alpha\sigma}^{GA} = \sum_{\Gamma\Gamma'} \frac{\sqrt{p_{i\Gamma} p_{i\Gamma'}} \left| \langle \Gamma_i | c_{i\alpha\sigma}^{\dagger} | \Gamma'_i \rangle \right|}{\sqrt{n_{i\alpha\sigma}^0 (1 - n_{i\alpha\sigma}^0)}} \qquad (12)$$

with $n_{i\alpha\sigma}^0 = \langle c_{i\alpha\sigma}^{\dagger} c_{i\alpha\sigma} \rangle_0$. The two-electron correlation matrix is approximated by the following factorized form,

$$\begin{aligned} \langle c_{i\alpha\sigma}^{\dagger} c_{j\beta\sigma'}^{\dagger} c_{l\delta\sigma'} c_{k\gamma\sigma} \rangle_{\mathrm{G}} &= \langle c_{i\alpha\sigma}^{\dagger} c_{k\gamma\sigma} \rangle_{\mathrm{G}} \langle c_{j\beta\sigma'}^{\dagger} c_{l\delta\sigma'} \rangle_{\mathrm{G}} \\ &\quad - \delta_{\sigma\sigma'} \langle c_{i\alpha\sigma}^{\dagger} c_{l\delta\sigma} \rangle_{\mathrm{G}} \langle c_{j\beta\sigma}^{\dagger} c_{k\gamma\sigma} \rangle_{\mathrm{G}} \end{aligned} \qquad (13)$$

The Hartree-Fock type factorization introduces errors in the calculations of inter-site Coulomb interactions. The errors are alleviated by the last sum-rule correction term E_{sr} in eq. (6), which effectively shifts the inter-site two-body terms to more accurate onsite evaluations. The prefactor $\lambda_{i\alpha}$ is determined by the weighted average of the relevant inter-site two-electron Coulomb integrals.

$$\lambda_{i\alpha} = -\frac{\sum_{j\neq i,\beta} u(i\alpha j\beta; i\alpha j\beta) R_{ij}^{-6}}{\sum_{j\neq i,\beta} R_{ij}^{-6}} \qquad (14)$$

where R_{ij} is the distance from atom j to atom i and R_{ij}^{-6} services as the weighting factor here. The exact form of the weighting factor is not crucial, as long as it decays sufficiently fast.

The minimization of the CMR total energy functional amounts to solve a coupled set of eigen-value equations to determine $|\Psi_0\rangle$ and $\{p_{i\Gamma}\}$, in a self-consistent way [32, 33]. The solution for $|\Psi_0\rangle$ is equivalent to Hartree-Fock approach with renormalized single-particle Hamiltonian, which scales as N^4 with the dimension of basis set orbitals N. The onsite configuration block $\{p_{i\Gamma}\}$ is solved atom by atom independently, with a linear scaling of the number of atoms. Therefore, the CMR method features a Hartree-Fock like scaling overall.

In our implementation, we use the QUAsi-atomic Minimal Basis-set Orbitals (QUAMBOs) [41] as the basis-set to represent the many-electron Hamiltonian of the system in our CMR calculations. The same QUAMBO basis set is also used in FCI calculations for comparison. The results from the CMR and FCI calculations are also compared with available experimental results. The QUAMBOs maintain maximally the atomic characters while preserve the occupied mean-field molecular orbital subspace, which encodes the favourable bonding environment effects. They have been shown to be good approximations to the multi-configurational self-consistent field-determined correlating orbitals, recovering a large percentage of the correlation energy [42]. Our CMR computational package uses an interface with PySCF to obtain the *ab initio* molecular Hamiltonians, the atomic orbitals and Hartree-Fock occupied molecular orbitals [43]. QUAMBOs are then constructed and the corresponding Hamiltonian is derived, which is subsequently solved within the CMR approach. For computational efficiency, we also replace the local onsite configurations $\{\Gamma\}$ by the Fock states generated based on QUAMBOs, which holds approximately owing to the dominance of the onsite density-density type interactions.

3. Results and Discussion

In our earlier publication [32-35], we demonstrated the satisfactory performance of the CMR approach in several small molecules. Here we aim to present a relatively more comprehensive assessment of the method on a larger set of molecules from the G2-test set [40]. The molecules in this test set come from the first three rows of elements in the periodic table and have reliable experimental data to compare. The results are presented in two groups: homonuclear dimers and heteronuclear molecules.

3.1 Homonuclear Dimers

We have calculated all the dimers with singlet ground states in the first three rows of the periodic table. Figure1 shows the binding and dissociation curves of the dimers. The calculated equilibrium bond length and formation energies are summarized in Table 1. The QUAMBOs adopted in the CMR and full configuration interaction (FCI) calculations are constructed based on restricted Hartree-Fock molecular orbitals expanded in terms of aug-cc-pVTZ basis set [44]. The available experimental data are also included for comparison.

For dimers with effective two valence electrons, such as H_2, Li_2 and Na_2, the CMR method produces potential energy curves in perfect agreement with the FCI results based on QUAMBOs. While the theoretical results agree very well with the experiment for H_2, the formation energy errors are about 0.01 Hartree per atom (Har/atom) for Li_2 and Na_2. The equilibrium bond lengths are also overestimated by 0.11 and 0.42Å, which can be attributed to the approximation that, inner semi-core shells of 1s orbital for Li and 2p orbitals for Na are treated as frozen core shells in the present QUAMBO-based FCI and CMR calculations. In fact, these semi-core shells are often required to be treated as valence electrons for accurate energies as discussed in the DFT pseudopotential or effective core potential community [45, 46].

Accurate potential energy curves of halogen dimers have been proven to be very difficult to produce by *ab initio* calculations [47, 48]. Remarkably, the results of F_2 and Cl_2 obtained from our CMR are in close agreement with QUAMBO-based FCI calculations. Both theoretical curves follow the experimental data very well. The CMR equilibrium bond lengths are quite accurate, with 0.02 and 0.04 Å of deviations for F_2 and Cl_2 respectively. The formation energy errors are also very small, 0.002 Har/atom for both F_2 and Cl_2. Overall, the CMR approach predicts satisfactorily the binding and dissociation behaviour for dimers with effective single bond, like alkali and halogen dimers.

The description of the dissociation behaviour of N_2 and P_2 involves highly open-shell atoms with three unpaired electrons and is rather challenging theoretically [49-51]. Yet, the CMR approach agrees very well with the QUAMBO-based FCI in the calculations of binding and dissociation curves of N_2 and P_2 dimers as shown in Figure 1. Both theoretical results are also close to experimental data, with about 0.04 Å or less for the equilibrium bond length deviations and less than 0.02 Har/atom for the formation energy errors.

The proper description of the C_2 dimer dissociation involves breaking a multiple bond, therefore is also a great theoretical challenge [51,52]. Nevertheless, the CMR approach consistently predicts reasonably accurate binding and dissociation energy curve compared to the QUAMBO-based FCI method. In comparison with experiment, the CMR calculation shows a small equilibrium bond length deviation of 0.05 Å and a formation energy error of 0.02 Har/atom.

3.2 Heteronuclear Molecules

We intended to benchmark the performance of the CMR method by comparing with the FCI calculations under the same QUAMBOs basis. Therefore, we focused on heteronuclear molecules of relatively small size, where QUAMBO-based FCI calculation is still affordable. The theoretical potential energy curves are shown in Figure 2, and equilibrium bond lengths and formation energies are summarized in Table 1.

For the heteronuclear dimers with an effective single bond, such as HF, HCl, LiH, LiF, NaCl and FCl, the CMR method performs very well in calculating the binding and dissociation curves, as shown by the comparison with the QUAMBO-based FCI results in Figure 2. Generally, the CMR calculated results also show very small errors of less than 0.01Å for equilibrium bond lengths and 0.01 Har/atom for the formation energies, when compared to the experimental data. The exceptions are LiF and NaCl, which show relatively large formation energy errors of 0.027 and 0.056 Har/atom, respectively. It can be attributed to the frozen core approximation in the QUAMBO-based FCI and CMR calculations as discussed previously.

The hydride polyatomic molecules H_mX_n, including H_2O, H_2S, NH_3, PH_3, CH_4, and SiH_4, represent a first set for benchmarking the CMR method in treating various geometrical environments with single polarized covalent bond. The theoretical total energies as a function of uniformly stretching H-X bond from the CMR calculations are in good agreement with the QUAMBO-based FCI results. The CMR equilibrium bond lengths and formation energies are also reasonably accurate, with the errors under 0.02 Å for the bond length and about 0.02 Har/atom for the formation energy in comparison with experiment.

Finally, the calculations of oxide molecules XO_m, including CO, CO_2 and SiO, demonstrate the quality of the CMR method in describing the formation and breaking of double polarized covalent bond. Indeed, the QUAMBO-based CMR and FCI calculations give quite consistent binding and dissociation curves for all of them. On a more quantitative level, the agreement between QUAMBO-based CMR and FCI is not uniform across the set of molecules. More detailed energy component analyses for the results will be necessary to identify the underlying reasons, which may lead to further improvement of the CMR approach.

It should be pointed out that the numerical calculations results of some molecules are not exactly the same as those reported in our early publication [32]. In principle, the minimal basis set orbitals in the CMR and FCI calculations can be variationally optimized. In the case of hydrogen molecule, it is found that the result from numerically optimized minimal basis-set orbitals is very close to the results obtained from the QUAMBO. For molecules like N_2, the numerical orbital optimization shows a bit bigger effect close to the atomic limit. As a result, some optimization for the QUAMBOs were carried out in the work of Ref.32. However, the orbital optimization incurs additional complications for the numerical simulation, while only introduces differences comparable or smaller than the mean errors of the methods when compared with experiments. Therefore, QUAMBOs which preserve the Hartree-Fock occupied space are used without further optimizations for all the present calculations.

4. Conclusions

We present a series of benchmark calculations of the CMR method on the G2 subset of molecules with spin-singlet ground state. The binding and dissociation energy curves are consistently in close agreement with FCI results using the same QUAMBOs basis, as well as the experimental measurements. The CMR method naturally applies to both finite molecules and infinite systems, as has been demonstrated in the recent calculations of periodic atomic hydrogen systems [33]. The physical reason of the good accuracy of CMR method in describing the total energies, especially in the dissociation process with increasing static correlation effects, is that the underlying Gutzwiller wave function explicitly takes the atomic many-body correlations into account, which guarantees the system evolves to proper atomic states subject to the Gutzwiller constraints on the local onsite density matrices. The residual correlation effects, such as nonlocal correlation and dynamical correlation effects beyond the CMR approach, might become increasingly important for systems with more electrons, including heavier elements and larger systems. The first approximate way to alleviate the residual correlation error is to introduce a correlation energy functional, with a form like local density approximation in DFT, which has been practiced in the recent publication [33]. The generalization of the CMR calculations to magnetism is straightforward. The effect of Gutzwiller constraints on magnetic calculations, which effectively confines the many-body manifold where the magnetic solution can search, is of interest and to be investigated.

Acknowledgements

This work was supported by the US Department of Energy(DOE), Office of Science, Basic Energy Sciences, Materials Science and Engineering Division including a grant of computer time at the National Energy Research Scientific Computing Centre (NERSC) in Berkeley. Ames Laboratory is operated for the US DOE by Iowa State University under Contract No. DE-AC02-07CH11358. HZ and WCL are supported by the National Natural Science Foundation of China (Grant No. 21773132).

References

[1] Landau L D, Lifshitz E M, Pitaevskii L P 1979 *Statistical Physics* Part 2, 3rd Edition (Course of Theoretical Physics, Volume 09), 2nd ed.

[2] Nozieres P *Theory Of Interacting Fermi Systems* 1997 Westview Press

[3] Purvis III G D, Bartlett R J 1982 A Full Coupled -Cluster Singles and Doubles Model: The Inclusion of Disconnected Triples *J. Chem. Phys.***76** 1910-1918

[4] Dykstra C, Frenking G, Kim K, Scuseria G 2005 *Theory and Applications of Computational Chemistry* Elsevier.

[5] Bartlett R J, Musiał M 2007 Coupled-Cluster Theory in Quantum Chemistry *Rev. Mod. Phys.* **79** 291-352

[6] Lyakh D I, Musiał M, Lotrich V F, Bartlett R J 2012 Multireference Nature of Chemistry: The Coupled-Cluster View *Chem. Rev.***112** 182-243

[7] Schmidt M W, Gordon M S 1998 The Construction and Interpretation of MCSCF Wavefunctions *Annu. Rev. Phys. Chem.* **49** 233-266.

[8] Sherrill C D, Schaefer III H F 1999 The Configuration Interaction Method: Advances in Highly Correlated Approaches *Adv. Quantum Chem.***34** 143-269

[9] Szalay P G,Müller T, Gidofalvi G, Lischka H, Shepard R 2012 Multiconfiguration Self-Consistent Field and Multireference Configuration Interaction Methods and Applications *Chem. Rev.* **112** 108-81

[10] Fehske H, Schneider R, Weiße A 2007 *Computational Many-Particle Physics*, Springer

[11] Austin B M, Zubarev D Y, Lester Jr. W. A 2012 Quantum Monte Carlo and Related Approaches *Chem. Rev.* **112** 263-288

[12] Berg E, Metlitski M A, Sachdev S 2012 Sign-Problem-Free Quantum Monte Carlo of The Onset of Antiferromagnetism in Metals *Science* **338** 1606-9

[13] Booth G H, Grüneis A, Kresse G, Alavi A 2013 Towards an Exact Description of Electronic Wavefunctions in Real Solids *Nature* **493** 365-370

[14] Kim J, Baczewski A, Beaudet T D, Benali A, Bennett M C, Berrill M A, Blunt N S, Borda E J e L, Casula M, Ceperley D M, Chiesa S, Clark B K, III R C C, Delaney K T, Dewing M, Esler K P, Hao H, Heinonen O, Kent P R C, Krogel J T, Kylänpää I, Li Y W, Lopez M Gm Luo Y, Malone F D, Martin R M, Mathuriya A, McMinis J, Melton C A, Mitas L, Morales M A, Neuscamman E, Parker W D, Flores S D P, Romero N A, Rubenstein B M, Shea J A R, Shin H, Shulenburger L, Tillack A, Townsend J P, Tubman N M, Goetz B V D, Vincent J E, Yang D C M, Yang Y, Zhang S, Zhao L 2018 QMCPACK: an Open Source *ab initio* Quantum Monte Carlo Package for The

Electronic Structure of Atoms, Molecules and Solids *J. Phys.:Condens. Matter* **30** 195901

[15] Motta M, Ceperley D M, Chan G K-L, Gomez J A, Gull E, Guo S, Jiménez-Hoyos C A, Lan T N, Li J, Ma F, Millis A J, Prokof'ev N V, Ray U, Scuseria G E, Sorella S, Stoudenmire E M, Sun Q, Tupitsyn I S, White S R, Zgid D, Zhang S 2017 Towards the Solution of The Many-Electron Problem in Real Materials: Equation of State of The Hydrogen Chain with State-of-The-Art Many-Body Methods *Phys. Rev. X* **7** 031059

[16] Anisimov V I, Zaanen J, Andersen O K 1991 Band theory and Mott Insulators: Hubbard U Instead of Stoner I *Phys. Rev. B* **44** 943-954

[17] Anisimov V I, Aryasetiawan F, Lichtenstein A 1997 First-Principles Calculations of The Electronic Structure and Spectra of Strongly Correlated Systems: The LDA+ U Method *J. Phys.: Condens. Matter* **9** 767-808

[18] Georges A, Kotliar G, Krauth W, Rozenberg M J 1996 Dynamical Mean-Field Theory of Strongly Correlated Fermion Systems and The Limit of Infinite Dimensions *Rev. Mod. Phys.* **68** 13-125

[19] Savrasov S Y, Kotliar G, Abrahams E 2001 Correlated Electrons in Delta-Plutonium within ADynamical Mean-Field Picture *Nature* **410** 793-795

[20] Kotliar G, Savrasov S Y, Haule K, Oudovenko V S, Parcollet O, Marianetti C A 2006 Electronic Structure Calculations with Dynamical Mean-Field Theory *Rev. Mod. Phys.* **78** 865-951

[21] Ho K M, Schmalian J, Wang C Z 2008 Gutzwiller Density Functional Theory for Correlated Electron Systems *Phys. Rev. B* **77** 073101

[22] Yao Y X, Wang C Z, Ho K M 2011 Including Many-Body Screening into Self-Consistent Calculations: Tight-Binding Model Studies with The Gutzwiller Approximation *Phys. Rev. B* **83** 245139

[23] Deng X, Wang L, Dai X, Fang Z 2009 Local Density Approximation Combined with Gutzwiller Method for Correlated Electron Systems: Formalism and Applications *Phys. Rev. B* **79** 075114

[24] Deng X, Dai X, Fang Z 2008 LDA+ Gutzwiller Method for Correlated Electron Systems *EPL-Europhys. Lett* **83** 37008

[25] Lanatà N, Strand H U R, Dai X, Bo H 2012 Efficient Implementation of The Gutzwiller Variational Method *Phys. Rev. B* **85** 35133

[26] Wang G, Qian Y, Xu G, Dai X, Fang Z 2010 *Phys. Rev.Lett.* **104** 047002

[27] Czyżyk M T, Sawatzky G A 1994 Local-Density Functional and On-Site Correlations: The Electronic Structure of La_2CuO_4 and $LaCuO_3$ *Phys. Rev. B* **49** 14211-14228

[28] Seo D-K 2007 Self-Interaction Correction in The LDA+ U Method *Phys. Rev.B* **76** 033102

[29] Karolak M, Ulm G, Wehling T, Mazurenko V, Poteryaev A, Lichtenstein A 2010 Double Counting in LDA Plus DMFT-The Example of NiO *J. Electron Spectrosc.Relat. Phenom.* **181** 11–15

[30] Haule K, Birol T, Kotliar G 2014 Covalency in Transition-Metal Oxides within All-Electron Dynamical Mean-Field Theory *Phys. Rev. B* **90** 075136

[31] Haule K 2015 Exact Double Counting in Combining the Dynamical Mean Field Theory and The Density Functional Theory *Phys. Rev.Lett.* **115** 196403

[32] Liu C, Liu J, Yao Y X, Wu P, Wang C Z, Ho K M 2016 Correlation Matrix Renormalization Theory: Improving Accuracy with Two-Electron Density-Matrix Sum Rules *J. Chem. Theory Comput.* **12** 4806-4811

[33] Zhao X, Liu J, Yao Y X, Wang C Z, Ho K M 2018 Correlation Matrix Renormalization Theory for Correlated-Electron Materials with Application to The Crystalline Phases of Atomic Hydrogen *Phys. Rev. B* **97** 075142

[34] Yao Y, Liu J, Wang C Z, Ho K M 2014 Correlation Matrix Renormalization Approximation for Total-Energy Calculations of Correlated Electron Systems *Phys. Rev. B* **89** 045131

[35] Yao Y, Liu J, Liu C, Lu W C, Wang C Z, Ho K M 2015 Efficient and Accurate Treatment of Electron Correlations with Correlation Matrix Renormalization Theory *Sci. Rep.* **5** 13478

[36] Gutzwiller M C 1965 Correlation of Electrons in ANarrow *s* Band. *Phys. Rev.* **137** A1726–A1735

[37] Kotliar G, Ruckenstein A E 1986 New Functional Integral Approach to Strongly Correlated Fermi Systems: The Gutzwiller Approximation as A Saddle Point *Phys. Rev.Lett.* **57** 1362-1365

[38] Bünemann J, Weber W, Gebhard F 1998 Multiband Gutzwiller Wave Functions for General On-Site Interactions *Phys. Rev. B* **57** 6896-6916

[39] Bünemann J, Gebhard F 2007 Equivalence of Gutzwiller and Slave-Boson Mean-Field Theories for Multiband Hubbard Models. *Phys. Rev. B* **76** 193104

[40] Curtiss L A, Raghavachari K, Redfern P C, Pople J A 1997 Assessment of Gaussian-2 and Density Functional Theories for The Computation of Enthalpies of Formation *J. Chem. Phys.* **106** 1063-1079

[41] Lu W C, Wang C Z, Schmidt M W, Bytautas L, Ho K M, Ruedenberg K 2004 Molecule Intrinsic Minimal Basis Sets. I. Exact Resolution of *ab initio* Optimized Molecular Orbitals in Terms of Deformed Atomic Minimal-Basis Orbitals *J. Chem. Phys.* **120** 2629-2637

[42] Lu W C, Wang C Z, Schmidt M W, Bytautas L, Ho K M, Ruedenberg K 2004 Molecule Intrinsic Minimal Basis Sets. II. Bonding Analyses for Si_4H_6 and Si_2 to Si_{10} *J. Chem. Phys.* **120** 2638-2651

[43] Sun Q, Berkelbach T C, Blunt N S, Booth G H, Guo S, Li Z, Liu J, McClain J D, Sayfutyarova E R, Sharma S, Wouters S, Chan G K L 2017 PySCF: The Python-Based Simulations of Chemistry Framework *WIREs Comput. Mol. Sci.* **8** e1340

[44] Dunning Jr T H 1989 Gaussian Basis Sets for Use in Correlated Molecular Calculations. I. The Atoms Boron through Neon and Hydrogen J. Chem. Phys. **90** 1007-1023

[45] Blöchl P E 1994 Projector augmented-wave method *Phys. Rev. B* **50** 17953

[46] Kresse G, Joubert D 1999 From ultrasoft pseudopotentials to the projector augmented wave method *Phys. Rev. B* **59** 1758

[47] Bytautas L, Matsunaga N, Nagata T, Gordon M S, Ruedenberg K 2007 Accurate *ab initio* Potential Energy Curve of F_2. II. Core-Valence Correlations, Relativistic Contributions, and Long-Range Interactions *J. Chem. Phys.* **127** 204301

[48] Laidig W D, Saxe P, Bartlett R J 1987 The Description of N_2 and F_2 Potential Energy Surfaces Using Multireference Coupled Cluster Theory *J. Chem. Phys.* **86** 887-907

[49] Li X, Paldus J 2008 Full Potential Energy Curve for N_2 by The Reduced Multireference Coupled-Cluster Method *J. Chem. Phys.* **129** 054104

[50] Piris M, March N H 2016 Potential Energy Curves for P_2 and P_2^+ Constructed from A Strictly N-Representable Natural Orbital Functional *Phys. Chem. Liq.* **54** 797-801

[51] Bytautas L, Scuseria G E, Ruedenberg K 2015 Seniority Number Description of Potential Energy Surfaces: Symmetric Dissociation of Water, N_2, C_2, and Be_2 *J. Chem. Phys.* **143** 094105

[52] Abrams M L, Sherrill C D 2004 Full Configuration Interaction Potential Energy Curves for The $X^1\Sigma_g^+$, $B^1\Delta_g$, and $B'^1\Sigma_g^+$States of C_2: A Challenge for Approximate Methods *J. Chem. Phys.* **121** 9211-9219

[53] Lemmon E W, McLinden M O, Friend D G, Linstrom P J, Mallard W G 2016 NIST chemistry WebBook, Nist Standard Reference Database Number 69, National Institute of Standards and Technology: Gaithersburg MD

[54] Darwent B D 1970 Bond Dissociation Energies in Simple Molecules, National Standard Reference Data System, National Bureau of Standards

[55] Musiał M, Kucharski S A 2014 First Principle Calculations of the Potential Energy Curves for Electronic States of the Lithium Dimer *J.Chem. Theory Comput.* **10** 1200-1211

[56] Matsunaga N, Zavitsas A A 2004 Comparison of Spectroscopic Potentials and An *a priori* Analytical Function. The Potential Energy Curve of The Ground State of The Sodium Dimer, $X^1\Sigma_g^+$ Na_2 *J. Chem. Phys.* **120** 5624-5630

[57] Colbourn E, Dagenais M, Douglas A, Raymonda J 1976 The Electronic Spectrum of F_2 *Can. J. Phys.* **54** 1343-1359

[58] Kokh D B, Alekseyev A B, Buenker R J 004 Theoretical Study of The UV Photodissociation of Cl_2: Potentials, Transition Moments, Extinction Coefficients, and Cl*/Cl Branching Ratio *J. Chem. Phys.* **120** 11549-11556.

[59] Huber K P, Herzberg G 1979 *Molecular Spectra and Molecular Structure*, Springer Science & Business Media: New York

[60] Dunning Jr T H 1976 The Low-Lying States of Hydrogen Fluoride: Potential Energy Curves for The $X\,^1\Sigma^+$, $^3\Sigma^+$, $^3\Pi$, and $^1\Pi$ States *J. Chem. Phys.* **65** 3854-3862

[61] Maul C, Chichinin A I, Gericke K H 2011 Multiphoton Ionization and Fragmentation of Hydrogen Chloride: A Diatomic Still Good for a Surprise *Journal of Atomic, Molecular, and Optical Physics* **2011** 410108.

Table 1. Summary of Equilibrium Bond Length R_0 and Binding Energy E_b of Test Set from *Ab Initio* Calculations on Various Methods with the errors measured in σ, ME and MAE[a]

	R_0(Å)			E_b (Har./atom)		
A_2	**QUAMBO-CMR**	**QUAMBO-FCI**	**Exp.**	**QUAMBO-CMR**	**QUAMBO-FCI**	**Exp.**
H_2	0.76	0.76	0.74	0.082	0.083	0.082
Li_2	2.78	2.89	2.67	0.004	0.007	0.020
C_2	1.29	1.24	1.24	0.092	0.105	0.114
N_2	1.10	1.10	1.10	0.181	0.176	0.178
F_2	1.43	1.44	1.41	0.027	0.021	0.029
Na_2	3.50	3.50	3.08	0.006	0.005	0.015
P_2	1.93	1.94	1.89	0.078	0.074	0.091
Cl_2	2.03	2.06	1.99	0.042	0.035	0.044
AB	**QUAMBO-CMR**	**QUAMBO-FCI**	**Exp.**	**QUAMBO-CMR**	**QUAMBO-FCI**	**Exp.**
LiH	1.60	1.58	1.60	0.035	0.032	0.045
CH_4	1.10	1.10	1.09	0.126	0.119	0.125
NH_3	1.03	1.01	1.01	0.128	0.107	0.110
H_2O	0.94	0.93	0.96	0.134	0.115	0.117
HF	0.93	0.92	0.92	0.103	0.101	0.109
SiH_4	1.51	1.49	1.48	0.113	0.095	0.097
PH_3	1.44	1.42	1.42	0.116	0.086	0.090
H_2S	1.32	1.32	1.34	0.107	0.087	0.092
HCl	1.27	1.26	1.27	0.090	0.078	0.082
LiF	1.55	1.54	1.56	0.083	0.083	0.110
CO	1.12	1.12	1.13	0.200	0.190	0.206
CO_2	1.20	1.20	1.16	0.211	0.180	0.204
SiO	1.52	1.51	1.51	0.173	0.126	0.150
FCl	1.64	1.65	1.63	0.048	0.034	0.049
NaCl	2.39	2.39	2.36	0.023	0.023	0.079
σ	0.09	0.10		0.018	0.012	
ME	0.03	0.04		-0.002	-0.012	
MAE	0.04	0.04		0.013	0.012	

[a]QUAMBO-CMR and QUAMBO-FCI results are compared with experimental data [40, 53-54] reported with the standard deviation σ and the Mean Error (ME), Mean Absolute Errors (MAE). The R_0 values for CH_4, NH_3, H_2O, SiH_4, PH_3 and CO_2 are equilibrium bond lengths of C−H, N−H, O−H, Si−H, P-H and C-O, respectively.

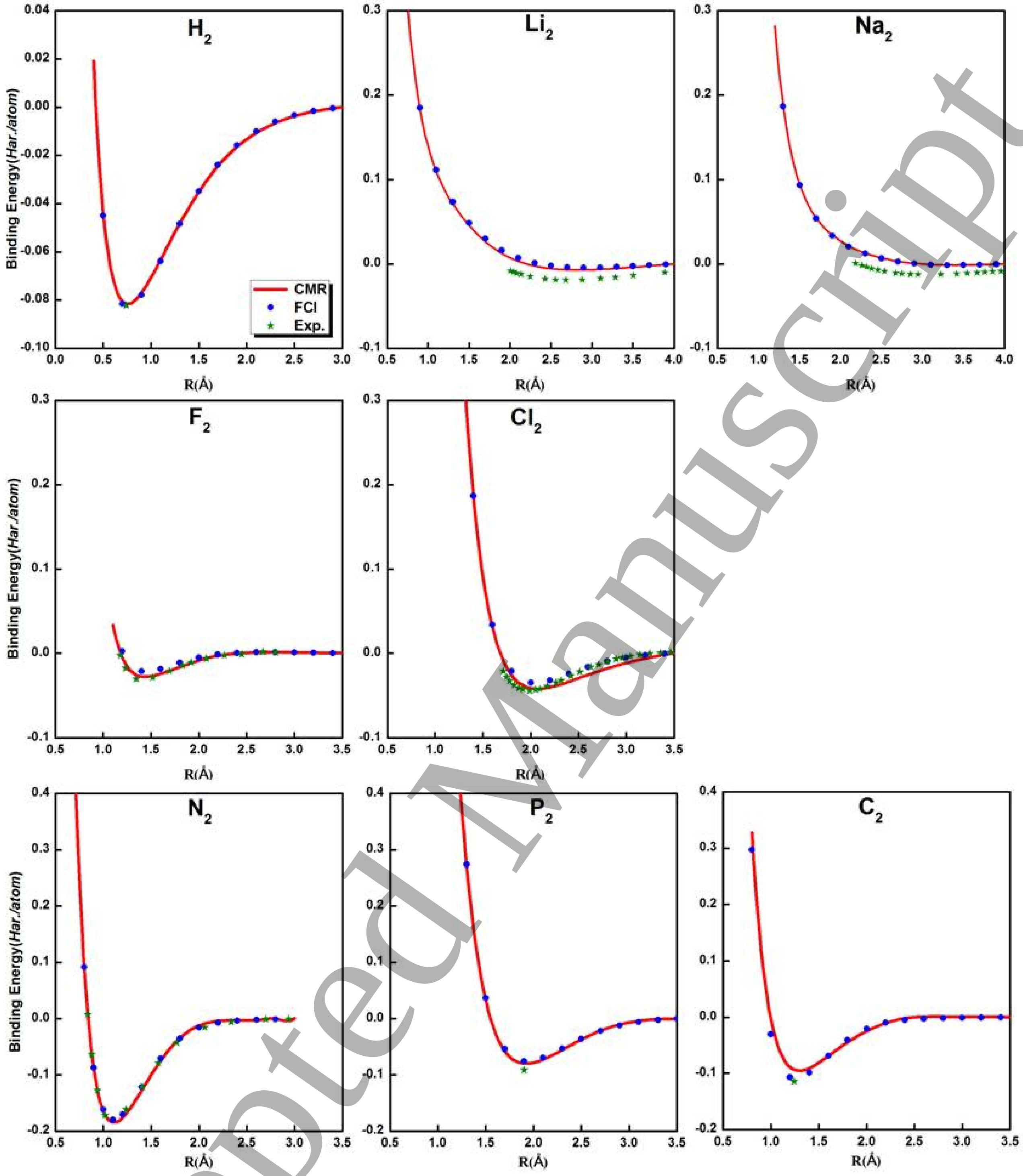

Figure 1. Potential energy curves of homonuclear dimers, including H_2, Li_2, Na_2, F_2, Cl_2, Na_2, N_2, P_2, and C_2. The CMR and FCI calculations are at QUAMBOs level which are constructed from the aug-cc-pVTZ basis-set. The available experimental data are included [53-59].

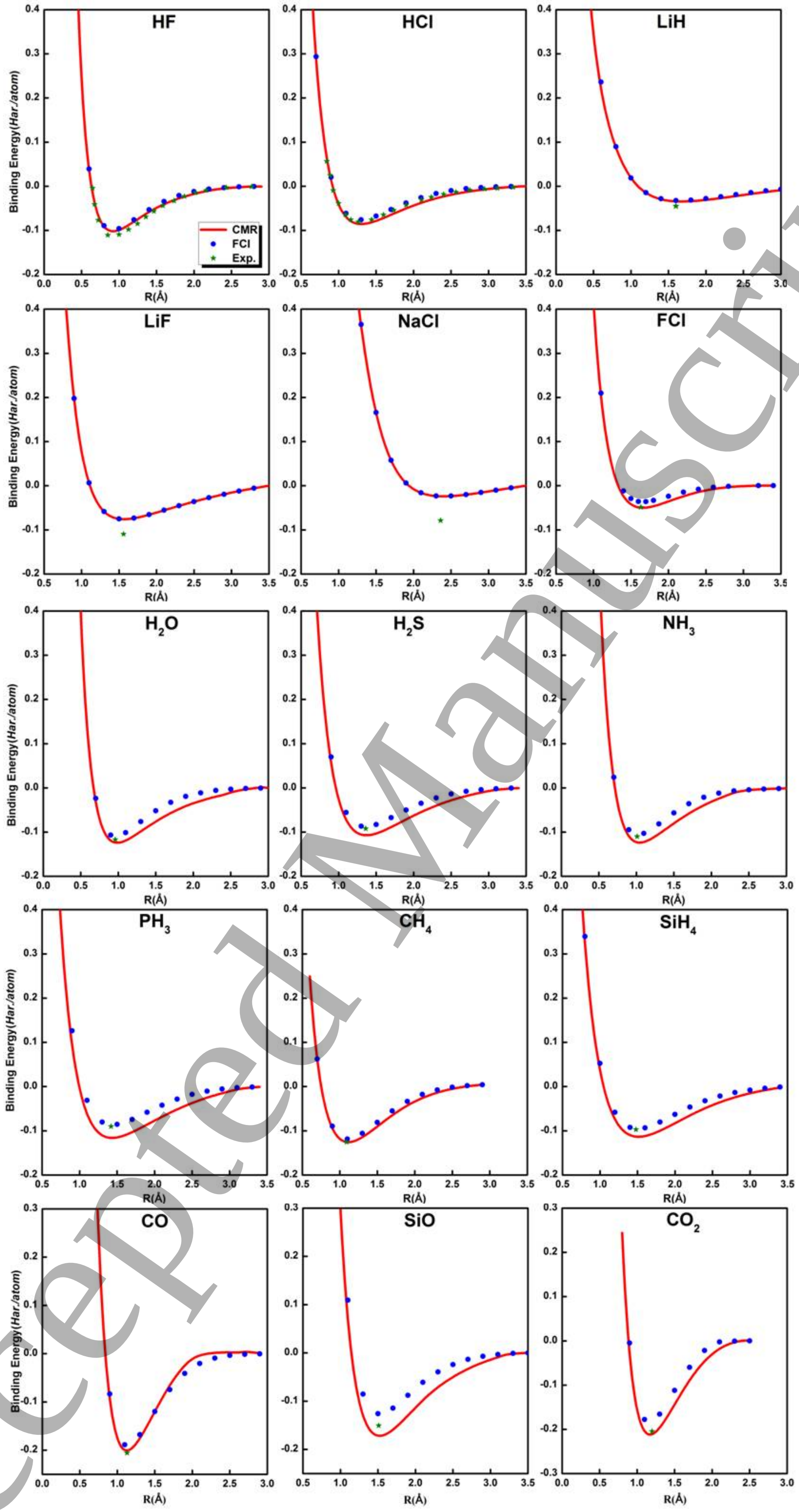
HF
HCl
LiH
LiF
NaCl
FCl
H2O
H2S
NH3
PH3
CH4
SiH4
CO
SiO
CO2
CMR
FCI
Exp.
Binding Energy(Har./atom)
R(Å)

Figure 2. Potential energy curves of heteronuclear molecules. The CMR and FCI calculations are based on the QUAMBOs constructed from the aug-cc-pVTZ basis-set. The available experimental data are included [53-54, 60, 61].